Particle Size Sampling and Object-Oriented Image Analysis for Field Investigations of Snow Particle Size, Shape, and Distribution

Susanne Ingvander‡*

*Ian A. Brown**

*Peter Jansson**

*Per Holmlund**

Cecilia Johansson† and

*Gunhild Rosqvist**

*Department of Physical Geography and Quaternary Geology, Stockholm University, S-106 91 Stockholm, Sweden
†Department of Earth Science, Uppsala University, Villavägen 16, SE- 752 36 Uppsala, Sweden
‡Corresponding author: susanne.ingvander@natgeo.su.se

Abstract

Snow particle size is an important parameter strongly affecting snow cover broadband albedo from seasonally snow covered areas and ice sheets. It is also important in remote sensing analyses because it influences the reflectance and scattering properties of the snow. We have developed a digital image processing method for the capture and analysis of data of snow particle size and shape. The method is suitable for quick and reliable data capture in the field. Traditional methods based on visual inspection of samples have been used but do not yield quantitative data. Our method provides an alternative to both simpler and more complex methods by providing a tool that limits the subjective effect of the visual analysis and provides a quantitative particle size distribution. The method involves image analysis software and field efficient instrumentation in order to develop a complete process-chain easily implemented under field conditions. The output from the analysis is a two-dimensional analysis of particle size, shape, and distributions for each sample. The results of the segmentation process were validated against manual delineation of snow particles. The developed method improves snow particle analysis because it is quantitative, reproducible, and applicable for different types of field sites.

Introduction

Snow particle size and shape analysis is a key ingredient in snow related investigations such as, for example, avalanche risk analysis (Lehning et al., 1999), ground control for remote sensing investigations of snow cover and its properties (Wiscombe and Warren, 1980; Nolin and Dozier, 1993, 2000; Dozier and Painter, 2004; Scambos et al., 2007; Dozier et al., 2009), and in accumulation modeling studies (Kirnbauer et al., 1994; Fierz et al., 2009). Traditionally snow particle studies have largely been accomplished using either visual observations in the field (following standards outlined in e.g. Fierz et al., 2009) or by gathering samples in the field for subsequent laboratory analysis (e.g. Albert, 2002; Gay et al., 2002). The visual observations have the benefit of providing direct results but are cumbersome and may involve some subjectivity and lower accuracy (Colbeck et al., 1990; Ingvander et al., 2010). The methods used for laboratory analysis typically involve fixating the sample in the field (requiring chemical techniques or specialist equipment) as well as transport of frozen samples to a laboratory for analysis (e.g. Albert, 2002; Gay et al., 2002, Matzl and Schneebeli, 2010). The laboratory techniques yield high-quality reproducible data but prohibit acquisition of results in the field and typically yield small sample sizes. Alternatively, sophisticated instrumentation using near infrared (NIR) imaging or specific surface area instruments can be used (e.g. Matzl and Schneebeli, 2006; Gallet et al., 2009), requiring increased logistical and financial support for the field campaign. Hence there is need for quick, reliable, and reproducible methods that combine the main advantages of both methods, the speed of visual field investigations, and the high-quality reproducible data of the laboratory methods. We have explored the advantages of using digital photography in combination with digital image analysis to record and analyze snow samples in the field.

Imaging of snow particle size has been carried out for different purposes and has evolved over time. This evolution has resulted from improving technology such as the introduction of charge-coupled devices and the digital camera (Mellor, 1965; Sommerfeld and LaChapelle, 1970; Colbeck et al., 1990; Grenfell et al., 1994; Pulliainen, 2006; Fierz et al., 2009). Lesaffre et al. (1998) presented a method for an objective analysis of particle size images extracting the mean convex radius of the snow particles. To improve on the two-dimensional analysis of images, the use of pore fillers were employed to fixate the pore space of the snow pack *in situ*, hence preserving the three-dimensional structure of the snow for later detailed analysis (Perla, 1982). Brun and Pahaut (1991) used iso-octane for fixation and post characterization of such snow samples. Such three-dimensional analysis provides rich data but is cumbersome to perform due to the fixation process and need for transport of larger samples to an environment where final analysis can be performed. Improving image analysis of snow particles thus provides a means to obtain good quality data in larger quantity and with little additional effort because the researcher is already in the field.

Earlier studies of snow particle size analysis in Dronning Maud Land, Antarctica, based on digital photography were made by, for example, Gay et al. (2002) and Kärkäs et al. (2002). Gay et al. (2002) focused on the methodology of snow sampling, providing three different types of analysis based on fixation with isooctane and sample analysis in a laboratory by using classical macro-photography and digital image acquisition. These studies show that photography-based methods are useful parts of any sampling and analysis program. A benefit of the digital images is that they can

easily be kept for posterity for re-analysis. Hence there is also a documentary benefit to an image based system.

We have modified, merged, and extended existing methods (Gay et al., 2002; Kärkäs et al., 2005) to arrive at the so-called Digital Snow Particle Property (DSPP) method, which requires a minimum of both instrument support and analysis time. The specific goal has been to provide opportunities for both quick field sampling and preliminary analysis, and subsequent re-analysis of the collected data using advanced image processing techniques. The method is based on digital photography of snow samples on a high-accuracy reference plate. The resulting images are processed in an object-oriented image analysis program yielding several parameters including snow particle size and shape. The result is a non-subjective method that yields statistical measures of the snow particle samples allowing for quantitative analysis and inter-sample comparison. Since the digital analysis is made using adjustable parameters, results can be double checked or re-analyzed with different settings at a later stage. The main limitation of the photographic method is that the analysis is two-dimensional. The data resulting from the analysis allow us to study the distribution within each sample and thereby enable comparisons between distributions from multiple samples. With our method we can obtain large quantities of field data with minimal equipment requirements and can provide quick and reproducible digital analysis of gathered data. This method can thus be used as a simple way to gain independent data for more complex studies of snow particle size. The novelty of this method in comparison with previous approaches is the use of a high-precision sampling grid for accurate pixel-size calibration and the pixel-based object-oriented image analysis method which enables analysis of multiple size parameters for a range of grains in each sample. This also enables us to establish size distributions for each sample and also minimizes the objective input by the observer in ordinary visual analysis. Furthermore, given the extremely large number of samples resulting, the DSPP approach facilitates the use of rigorous statistical analyses of the particle size data in contrast to approaches that focus on single grains or limited sample sizes.

In this paper we have chosen to use the term snow *particle* size rather than snow *grain* size for the objects we study. A snow grain is normally a single crystal (e.g. Fierz et al., 2009), though multiple crystal examples have been observed (e.g. Rolland du Roscoat et al., 2011). Furthermore, snow metamorphoses *in situ* as molecules transfer between individual grains in contact resulting in the bonding of grains across flat surfaces (Colbeck, 1998; Rolland du Roscoat et al., 2011). Thus, we have therefore opted to use the more general term particle to indicate that we do not distinguish between objects consisting of single grains (or crystals) or multi-grain bonded particles. These different grain types are very difficult to distinguish using traditional visual or other *in situ* methods and require appropriate and detailed instrumentation for determination.

Observations of grains *in situ* and in laboratory environments, using different observation techniques, have led to the development of a wide range of descriptive parameters. Different parameters used to describe snow particle sizes include: grain radius (Wiscombe and Warren, 1980), mean convex radius (Fily et al., 1997), and optically equivalent radius (Nolin and Dozier, 1993; Painter et al., 2007). Increasingly, Specific Surface Area (SSA) is becoming a favored parameter (Legagneux et al., 2002; Domine et al., 2008; Picard et al., 2009; Jacobi et al., 2010). The SSA of snow is used in optical equivalent analysis of snow grain size as it is strongly correlated to the spectral reflectance, an important factor in remote sensing of snow (Domine et al., 2008; Painter et al., 2009; Gallet et al., 2009). The SSA parameter normalizes the surface area to the snow particle volume as SSA is a relation between the surface area and the mass of a snow grain (Picard et al., 2009). A plethora of SSA approaches have been implemented. SSA has been measured by extracting snow samples and placing them beneath a near-infrared laser and measuring diode in an integrating sphere (e.g. Gallet et al., 2009). In contrast, Legagneux et al. (2002) measured snow SSA using methane absorption at the temperature of liquid nitrogen (77.1 K) in the laboratory. Matzl and Schneebeli (2010) compared gas absorption, standard micro X-ray tomography, and stereological analysis of vertical thin sections using micro X-ray tomography to validate the latter. This latter approach required the estimate of three-dimensional SSA from two-dimensional data, an approach with some relevance for the method described below. That said, the aim of the method presented here is to improve and reduce subjectivity in visual analysis of snow particles and not duplicate or replace existing highly sophisticated methods such as the measurement of specific surface area in the laboratory or the use of highly specialized equipment.

The Digital Snow Particle Property (DSPP) Method

The DSPP method was developed to meet our needs for fast, on-the-fly sampling and measurement, and for an efficient processing method for field determination of sampled surface snow particle sizes during the Swedish Japanese Antarctic Expedition 2007/2008 (Ingvander, unpublished data). There was a need to be able to gather information in a short time period since sampling could only be managed during brief stops of the traverse vehicles. The time constraints made accurate manual observations difficult. We also wished to make a large number of observations along the traverse, which precluded the use of the traditional sampling methods requiring samples to be carried back to a laboratory for analysis. In addition, we also aimed at gathering as much information as possible about not only size but also shape of the snow particles. The use of digital photography hence provided most of the positive aspects of the established sampling techniques. The speed of the field sampling and recording of samples in the field greatly limited the time available for sublimation that could have changed particle size and shape (e.g. Fujii and Kusunoki, 1982; Albert, 2002; Déry and Yau, 2002; Neumann et al., 2009. Although most of the details of the analysis lie in the digital image analysis, here we describe the entire workflow of the method. A digital analysis for particle size estimates consists of three main steps: (1) digital image acquisition of the particles to be analyzed; (2) digital analysis of the images; and (3) statistical analysis of the retrieved data. The complete workflow of the DSPP method is displayed in Figure 1.

Our field sampling instrumentation system consisted of a Canon EOS 350D digital camera mounted on a tripod that fixed the camera inside a transparent squared wind shelter (Fig. 2). An μm-accurate millimeter dot grid reference plate was used to support image calibration and rectification of the image during post-pro-
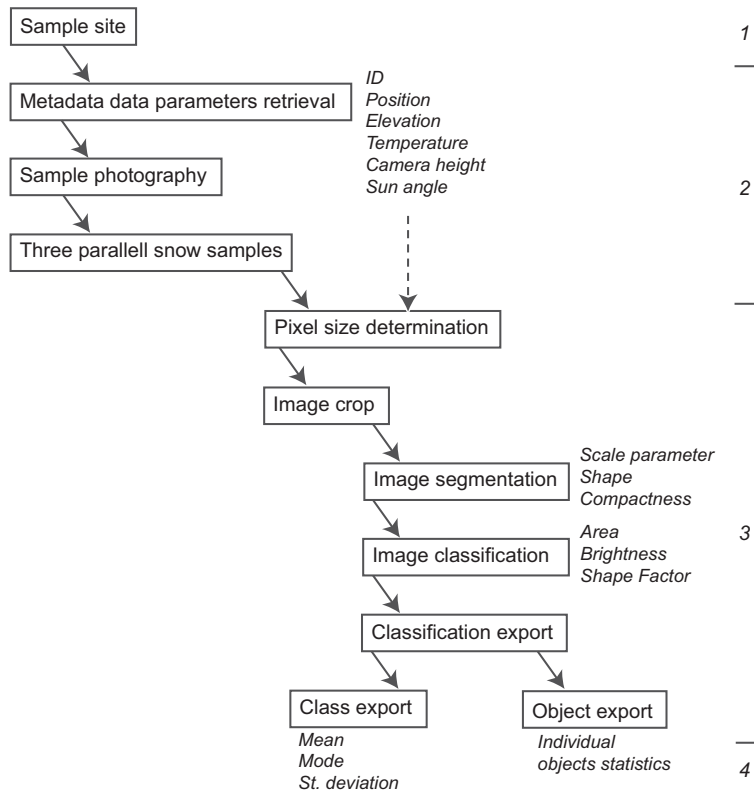
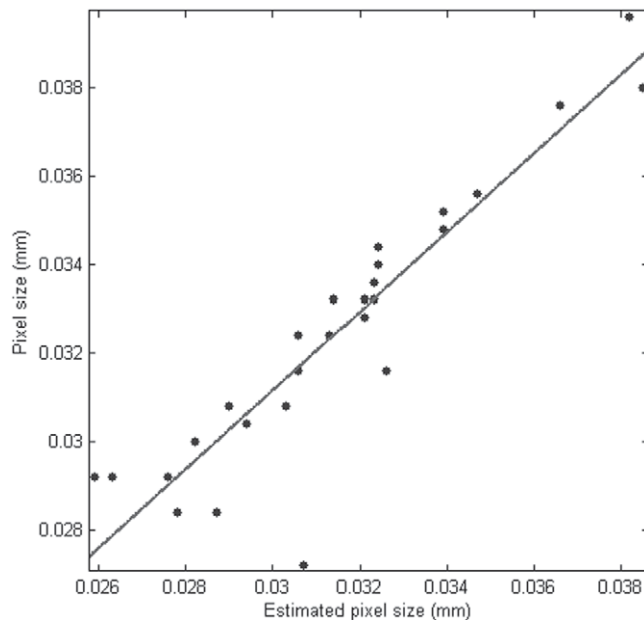FIGURE 1. Flowchart of the digital snow grain properties (DSPP) method. See text for details.

FIGURE 2. Scatter plot of equation-derived pixel size (estimated pixel size) (from correlating camera elevation and pixel size for sample images) and actual pixel size (pixel size) derived by implementing Equation (1) for 27 grid samples during the Japanese Swedish Traverse 2007/2008. $R^2 = 0.84$ and root mean squared error (RMSE) = 0.0012.

cessing. A snow sample was collected from the natural snow cover using a silicon spatula and placed on the reference plate by a gentle shake to disperse the particles over the glass plate. The plate was immediately photographed to prevent melting and/or sublimation. The image resolution was calculated in two different ways based on the sampling procedure: either by recording the distance between the camera and the sample glass (camera height) in order to calculate the pixel size in the images, or by counting the number of pixels between the millimeter markers on the reference plate.

The image analysis is performed by object-oriented image analysis software; we used Definiens Developer 7.0 in our study. The digital analysis is based on segmentation to identify each snow particle as an object and then apply different algorithms to extract a series of generic parameters such as width, length, area, circumference, etc. The result of the analysis is a comprehensive data set of all measures for all identified objects. No additional light source was added to the sample equipment as sufficient natural lighting was present and generated adequate contrast between the snow particles and the background in the images.

The object-oriented image analysis extracts every object in the images generating a size range and distribution within each sample. This enables statistical analysis of the size distribution within each sample generating exact size ranges, in contrast to visual/manual classification systems that generate a mean size within fixed size ranges for each class. Measured snow particles are thus binned based on the resolution of the image and the size of the objects to visualize size distribution.

The extraction of the sample from the snowpack using a spatula may result in the destruction of bonds between grains in some

cases. Obviously, care must be taken during sample extraction. This potential limitation to the method can be addressed in a number of ways. Visual inspection of the photographs can be used to assess the validity of the grain size distribution and maximum and minimum particle size thresholds adjusted to exclude extraneous objects. The image may be subset to remove regions that clearly exhibit damaged particles. Multiple samples and images are typically taken to improve the data quality and the very large number of particles resulting from the analysis, and the potential to use sophisticated statistical analyses *post prioi* means that the effects of damaged samples can be ameliorated.

In the following we will outline the digital processing steps and the resulting measures of particle size and shape. This is important since we need to show how our measures tie to standard methods for snow particle analysis.

A Brief Overview of Digital Image Analysis

Object-oriented image analysis involves applying a series of image processing operations to the images as described in the following processing chain and visualized in Figure 1.

IMAGE PREPARATION

The digital analysis requires a pixel-based sharp digital image. In this study we used JPEG and RAW formats. Note that JPEG compression is destructive, and these effects have to be considered. The image must first be cropped in image processing software in order to remove the reflective border areas of the calibration glass plate and to remove areas exhibiting snow particle clustering (multiple particles in aggregates), melt features, or frost tracks on the glass.

IMAGE RESOLUTION

The resolution (mean pixel size) (S_p) of each image is calculated by counting the number of pixels between each millimeter marker on the sampling grid in four directions (0, 90, 180 and 270°) at three markers $(P_1, P_2,$ and $P_3)$ in each image [Equation (1)] (step 2 in the DSPP method).

$$\bar{S}_p = \frac{P_{tot} l_{max}}{\sum_{i=1}^{4} d_{P_1}^i + \sum_{i=1}^{4} d_{P_2}^i + \sum_{i=1}^{4} d_{P_3}^i} \quad (1)$$

where P_{tot} is the total number of points where the numbers of pixels were counted, and l_{max} is the number of pixel distances counted. By dividing 1 mm by the total number of pixels divided by the number of pixel distances counted we receive the resolution of the image. For extensive data sets with registered camera elevation, the pixel resolution can be calculated by correlating the camera elevation with pixel resolution for reference images and implementing the equation on remaining images. Figure 3 shows an example of equation-derived pixel size and actual pixel size derived by using Equation (1) generating a root mean square (RMS) error of 0.0012.

SEGMENTATION

Using Definiens Developer 7.0 we segmented, then classified the snow particles. Definiens Developer image segmentation and
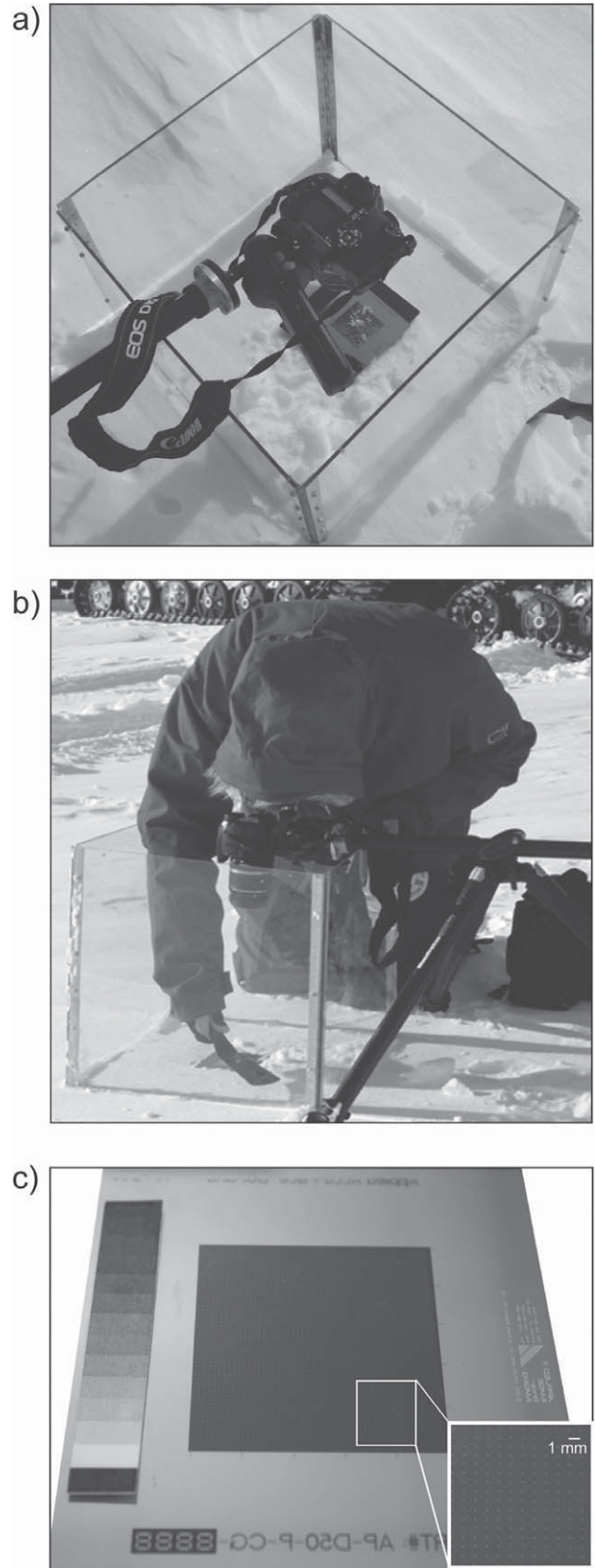
FIGURE 3. Field implementation of the instrumentation for using the DSPP method. (a) The fixed camera and the sample glass underlain by a dark reference plate to improve contrast; (b) example of surface snow sampling for photography; and (c) the micrometer accurate dot grid used. It is here equipped with a gray scale for light condition comparison.

classification have been used in a range of image processing applications (Benz and Pottier, 2001; Schiewe, 2002; van der Sande et al., 2003; Benz et al., 2004). In the following we focus on the Definiens Developer 7.0 software parameter definitions; all information below is based on this source unless otherwise stated. The segmentation and classification processes are integral to the program and are described fully in the Definiens user manual (Definiens, 2008) and, with emphasis on the segmentation process, in Baatz and Schäpe (2000). First the image is segmented using a multi-resolution segmentation algorithm in order to extract discrete objects in the image (Figs. 1 and 4). Multiple-resolution segmentation is performed grouping homogeneous pixels into regions from an evenly spaced set of seed cells in the image using user-defined segmentation parameters (Definiens, 2008). Multiresolution segmentation operates at multiple scales, thereby avoiding bias related to segment size. In the first run, each pixel is considered as being a seed cell. Pixels are then merged with surrounding pixels with the same attributes as defined by the segmentation parameters chosen (Baatz and Schäpe, 2000). The grouped pixels are then pairwise merged into regions in iterations that continue until no further merg-
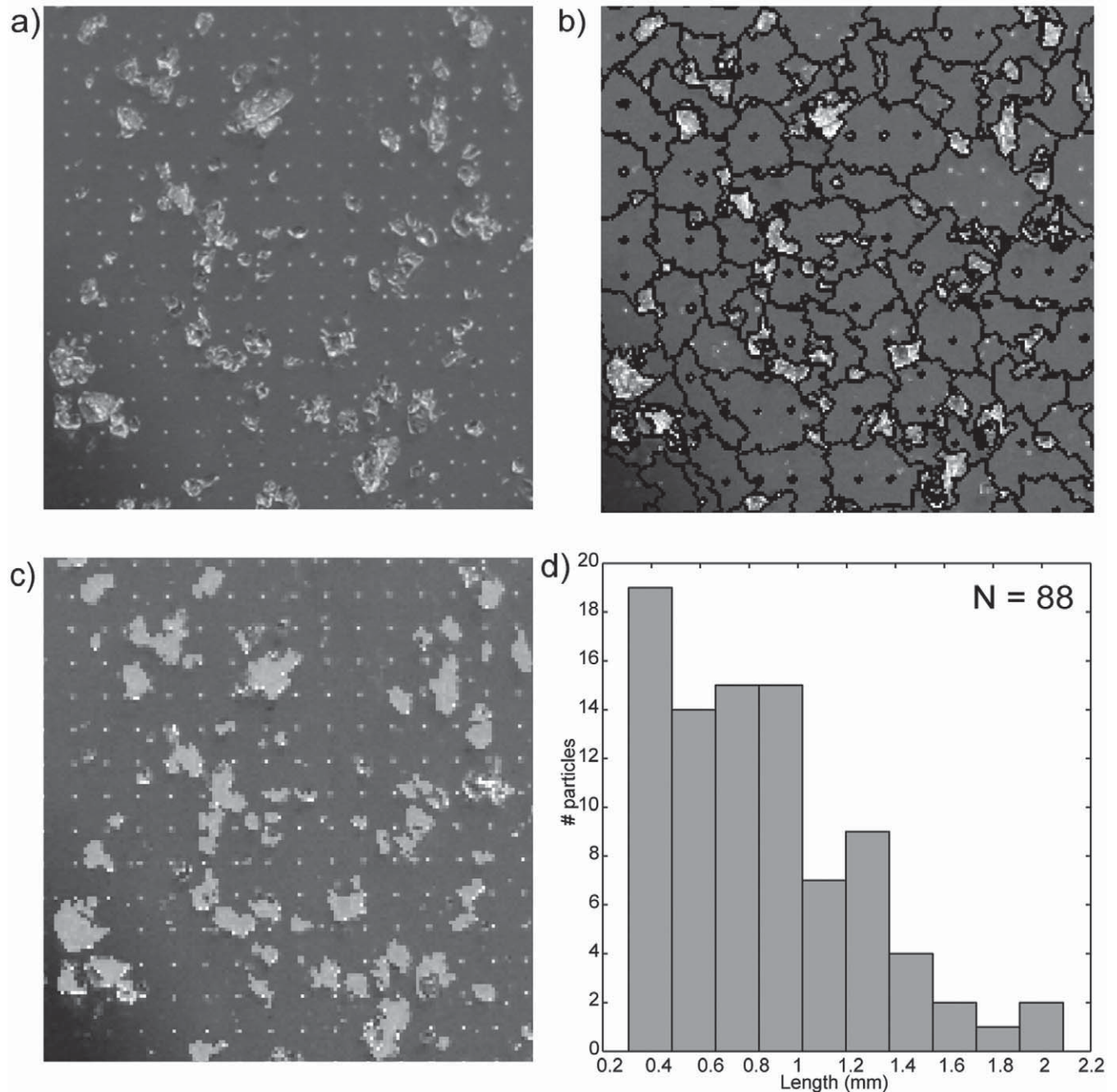

FIGURE 4. Examples of the image analysis processes: (a) raw image, which has been cropped to reduce size and increase particle visibility; (b) image after segmentation; (c) the segmented image after classification identifying segments corresponding to particles; and (d) resulting distribution from the classified image (note that the distribution shape is poor due to the low number of particles ($N = 88$) in the sample image.

ing is possible according to the given rule set (this is the so-called multiresolution approach). The limiting factor for the merge (resolution) is based on the scale parameter set by the user which is, in turn, based on the pixel size of the image. Higher scale parameter values generate larger, more diverse objects compared to a smaller scale parameter generating small homogeneous parameters. Segmentation parameters are chosen in order to capture the features in the image but constrained so as not to divide the objects to be analyzed into smaller features. The original image is segmented by two types of segmentation values: the shape, which determines to what level (in percent) the shape of the object contributes to the homogeneity of the image; and the compactness, which is a function of the homogeneity within the brightness and color of the objects (smoothness and compactness). To summarize, when the shape is set to 1, the segmentation is optimized for the shape of the objects, whereas if the segmentation is set to 0, the segmentation is optimized for the compactness and smoothness of the objects in the image. Testing and validation is appropriate when selecting these parameters.

CLASSIFICATION

The segmented images are classified by: (1) brightness, to contrast the snow particle against the background; (2) area, to reduce the influence of clusters and remove the millimeter markers; and (3) shape index, to determine the shape of the particle and remove elongated reflections in the sampling glass. This operation is performed by assigning a class with relevant threshold values for the objects to be extracted. The snow class was determined by extracting minimum and maximum values for snow particle objects and determining the threshold at multiple levels, including small snow particles and excluding clusters of particles. The classification is mostly consistent, but occasionally the brightness has to be adjusted for incident light in the image or the air content in the particle, which affects the transparency of the particles. The size range may also be adjusted for the presence of particles of extreme sizes. The minimum area value used in the classification of snow particles was 0.015 mm^2, which is just larger than the size of the millimeter markers of the sampling grid. The segmentation and classification values vary with snow and sample type, and values for the different regions are presented in Table 1. The segmented-classification pro-

cessing can be automated or, if necessary, run interactively to allow the images to be re-segmented by changing parameter settings.
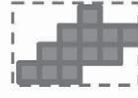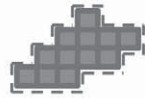
PARAMETER RETRIEVAL

The size of the objects classified as snow particles are calculated by identifying separate objects and using generic shape algorithms. The parameters are divided into different levels (I–III) based on how complex the calculations of the required parameter are (how many of the prior calculations are necessary in the calculation) (Fig. 5).

Based on the first-level data (I), size and shape parameters can be calculated by the level II and III algorithms. The most basic shape parameters are border length (*BL*) and area (*A*). As the pixel resolution is set initially in the program, the area is calculated using the area of each pixel (A_p) times the number of pixels in each object (n_p). The border length is simply the perimeter of each particle. Further algorithms at the basic level are the bounding box and eigenvalue calculations. The bounding box (*BB*) is the smallest rectangular area that encloses the object of interest. The geometrical definition is the difference between maximum and minimum coordinates in *x* and *y* direction for each object (Fig. 5). The final algorithm on level I is based on a tilted bounding box delimited by eigenvalues (ε) derived from the spatial distribution of the object. At the second level of calculations, the calculations are based on the values from the first level equations. An example of second level equations is length/width ratio, which is calculated using *BB* and ϵ: the ratio between the longest and the shortest axis is calculated for both *BB* and ε; the smallest value is the featured value. The largest enclosed ellipse (*LEE*) and smallest enclosing ellipse (*SEE*) are based on the eigenvalues and an ellipse with the same area as the object *OE*. The *OE* is downscaled in order to be completely surrounded by the object *LEE* or upscaled to surround the object *SEE*. The returned result is the ratio between the radius of the original ellipse and the radius of the *SEE* or *LEE* ellipse. This value explains the complexity of the object. The third level of equations is based on the results of the level II equations. As the smallest feature of *BB* and ε is determining the length-to-width ratio, the values retrieved (depending on which is the smallest) are the length and width, respectively. The DSPP method has been tested in different environments to verify its applicability outside of

TABLE 1

Five different rules sets of segmentation and classification systems used in Definiens Developer 7.0 to optimize grain size retrieval on four separate field sites where segmentation scale determines the size of the segmented objects, the compactness, and shape determined the spectral or spatial homogeneity of the objects. The classification values of area, brightness, and shape of the objects determine snow particle or not snow particle.

Region	Segmentation values			Classification values		
	Scale	Compactness	Shape	Area (mm^2)	Brightness (8 bit relative scale)	Shape
Antarctica coast	50	0.4	0.6	0.025–13.6	136–255	0–2.6
Antarctica plateau	50	0.4	0.6	0.015–13.6	145–255	0–2.6
Järämä 1	150	0.4	0.6	0.035–20	116–255	0–2.6
Järämä 2	50	0.2	0.8	0.035–20	116–255	0–2.6
Tarfala	30	0.4	0.6	0.035–13.6	200–255	0–2.6

Level I

Border length (BL)
BL= P x no outer pixel sides.

Area (A)
Area of snow grain.
$A = P^2 \times \#P_v$

Bounding box (BB)
Smallest rectangular area that encloses all pixels along X and Y axis.
$$BB = (\max X - \min X) \times (\max Y - \min Y)$$

Eigen values (EV)
Smallest rectangular area based on a tilted box and covariance mat

$$x_{center} = \frac{1}{\#P_v} \sum (x,y)^x$$

$$y_{center} = \frac{1}{\#P_v} \sum (x,y)^y$$

Level II

Length width ratio (LW)
Computed by BB and EV. Smallest value is the feature value.

$$\frac{L}{W} = smallest\_of\_\gamma^{EV} and\_\gamma^{BB}$$

$$\gamma_{v^{EV}} = \frac{\lambda_1(v)}{\lambda_2(v)} \qquad \gamma_{v^{BB}} = \frac{(k_{v^{BB}})^2}{\#P_v}$$

Largest enclosed ellipse (LEE)
Radious of the largest encapuslated ellipse in the object.

$$\varepsilon_v(x_0,y_0) with(x_0,y_0) = \max \varepsilon_v(x,y), (x,y) \in P_v$$

Level III

Length (L)
Polygons longest axis based on the L/W ratio estimation.

$$L = \sqrt{\#P_v} \times \gamma_v$$

Width (W)
Polygons shortest axis based on the L/W ratio estimation.

$$W = \frac{\#P_v}{\lambda_v}$$

FIGURE 5. Basic and derived parameters in Definiens Developer 7.0 used for generating snow particle size parameter data sets from collected images (Definiens, 2008). See text for a detailed description.

Antarctica for which it was originally designed. We will therefore briefly summarize our experiences from case studies.

Processing Examples

The method has so far been used at three very different sites: Dronning Maud Land, Antarctica (Ingvander et al., 2010), as well as Järämä (Ingvander et al., 2012) and Tarfala in northern Sweden (Ingvander et al., 2013). The Antarctic data set consists of 62 surface samples, ten 1-m pits sampled with 10-cm resolution, and 4 grid net samples (9 samples in a squared grid with 10-m resolution) along the Japanese Swedish Traverse 2007/2008 (JASE). The Järämä data set, consisting of surface and pit samples, was collected for a comparison between DSPP method results and a long-term monitoring data set collected by Abisko Scientific Research Station using their simplified classification system (Ingvander et al., 2012). The Tarfala data set was collected on Storglaciären, a glacier in the northern Swedish mountains where long-term snow studies have been performed as part of the ongoing mass balance program (e.g. Jansson and Pettersson, 2007), as part of a high-resolution study of seasonal snow accumulation (Jansson et al., 2007). The

data explored by us thus span several different types of snow regimes from high elevation subarctic mountains to forest snow cover as well as the extreme Antarctic snow conditions. Data from all three field sites have been used in order to develop and improve the method.

All data from the three sites have been collated and plotted as size distributions in Figure 6 in order to illustrate the differences in snow particle size between the three sampling sites. Segmentation and classification parameters, *rule sets*, for Antarctica and for coastal and polar plateau areas (Järämä and Tarfala) are presented in Table 1. The snow sampled at Järämä consisted of snow with widely different particle sizes, which required analysis with different rule sets (Ingvander et al., 2012).

The difference in brightness values is caused by the occurrence of melt features when sampling at temperatures above 0 °C and differences in lighting conditions during the different sampling sessions. Figure 7 shows the size distribution within each group of samples. The number of objects analyzed in each field campaign is also evident and depends on the sizes of the snow particles in each sample (small particle sizes allow more objects to be analyzed in each sample). Despite the number of particles in each distribu-
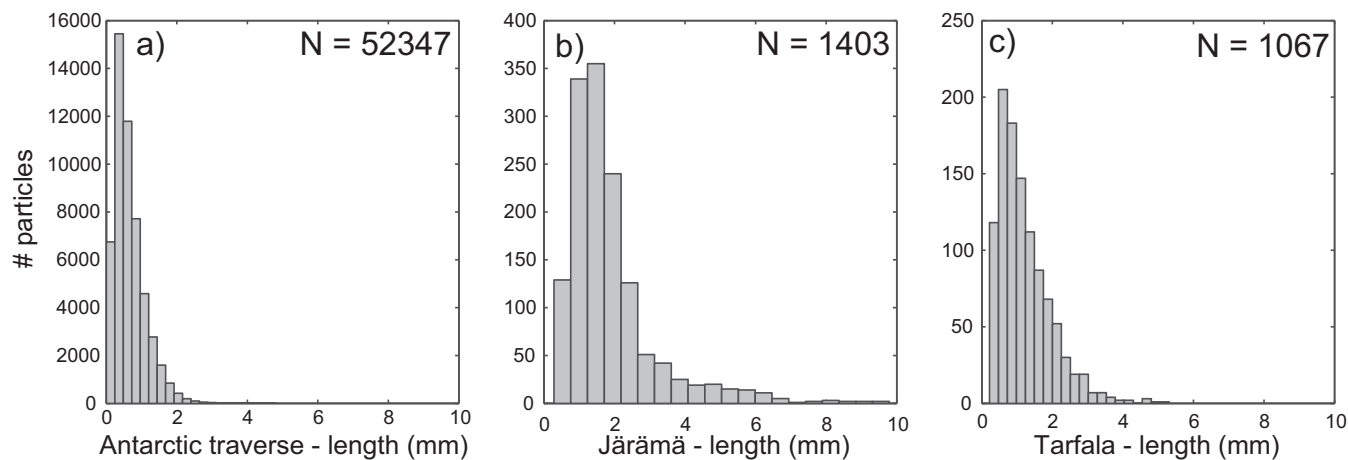
FIGURE 6. Snow particle size distributions from (a) Antarctica; (b) Järämä; and (c) Tarfala. See text for a discussion.

tion, there is a distinct negative skewness in all distributions. We will discuss this further below. Two examples of different snow size samples are presented in Figure 7.

The original sample 1 image of rounded particles (Fig. 7, part a) are segmented and classified according to Järämä 2, whereas the original sample 2 image of depth hoar (part b) is classified using the rule set of Järämä 1. The length results from the classified images (parts c and d) were binned using the maximum object size divided by the resolution for each image. The objects are binned separately according to resolution and object sizes. The bin sizes used in Figure 7 are 14.66 in part e and 15.57 in part f in the size distribution histograms. The interpreted size from visual observation and the mean DSPP size is presented in Figure 7. The results show that visual interpretation may overestimate sizes of small particles and underestimate the size of larger particles. Since the segmentation and classification is automatic, clustered particles may enter the distribution. This is the reason for the long distribution tail toward larger particle sizes (Fig. 7). This means that some caution must be made when using a distribution to assign a particle size value. The mode provides the dominant value while the mean is affected by the tail.

In order to test the reproducibility, a re-analysis where images were rotated 90° was made, which generated slightly deviating results. This deviation is caused by the software analysis algorithm. The software scans the image in a predetermined way; if altering the image orientation, the seed cell positions are altered, which means the segmentation develops differently. To obtain a length, the Definiens Developer 7.0 software uses either the bounding box or the eigenvalues as a basis for the calculation (Fig. 5). A rotation of the object may thus result in a switch of base parameter for the calculation of length, which may introduce smaller deviations. Figure 8 shows how the length and area parameters change when rotating the image.

The area does not show any appreciable deviations ($R^2 = 0.99$), but there is a deviation in length for the larger particle sizes although the correlation is still good ($R^2 = 0.97$). This behavior originates from the fact that area comes from a first-level equation, but length is calculated from a third-level equation (Fig. 5). The length parameter is based on the relation between the bounding box and eigenvalues through a derived length/width ratio value.

We deem this deviation of little significance, but it indicates how important knowledge of software algorithms can be. The difference in mean of area, length, and width is presented in Table 2.

We validated the method against visual interpretation using manual digitalization of snow particles and compared the size of the manually digitalized snow particle sizes with the DSPP-method retrieved particle sizes generating a $R^2 = 0.98$ and *RMSE* of 0.071 for the length parameter (Fig. 9).

It is important that the DSPP results are comparable to other investigations. The length parameter is comparable to the *International Classification of Seasonal Snow on the Ground* (Colbeck et al., 1990; Fierz et al., 2009) where the definition of snow grain size is the greatest extension of the grain. When identifying the average particle size we believe the mode from our distributions is to be compared with the particle size concept of the snow classification. Furthermore, the size parameters can be used to calculate the geometry of the objects and thereby determine the shape of the particles in the samples. For example, the length/width ratio can be used to determine the shape of the objects classified as snow particles. This shape parameter can be used to analyze morphology and shape altering processes such as wind transport (Kikuchi et al., 2005). Furthermore, shape differences may be useful in remote sensing applications (Mätzler, 1996).

Discussion and Recommendations

The DSPP method seems to successfully fulfill the basic requirements for analyzing snow particle size in the field. The method is cost effective, accurate, and delivers the size range (distribution) for each sample. It is an extension of existing methods using commercial instrumentation and software, which enables reproducibility within the scientific community. The developed DSPP method facilitates objective analysis of data from different types of snow and geographical regions. By introducing a completely automatic method, comparison of different data sets is possible independent of the analyzer. The method generates extensive data sets that improve the data that can be extracted and thereby offers a range of alternative measurements. The number of data points retrieved also improves the statistical reliability. Studying the distribution of the data shows a negative skewness in Figure 6. This information im-

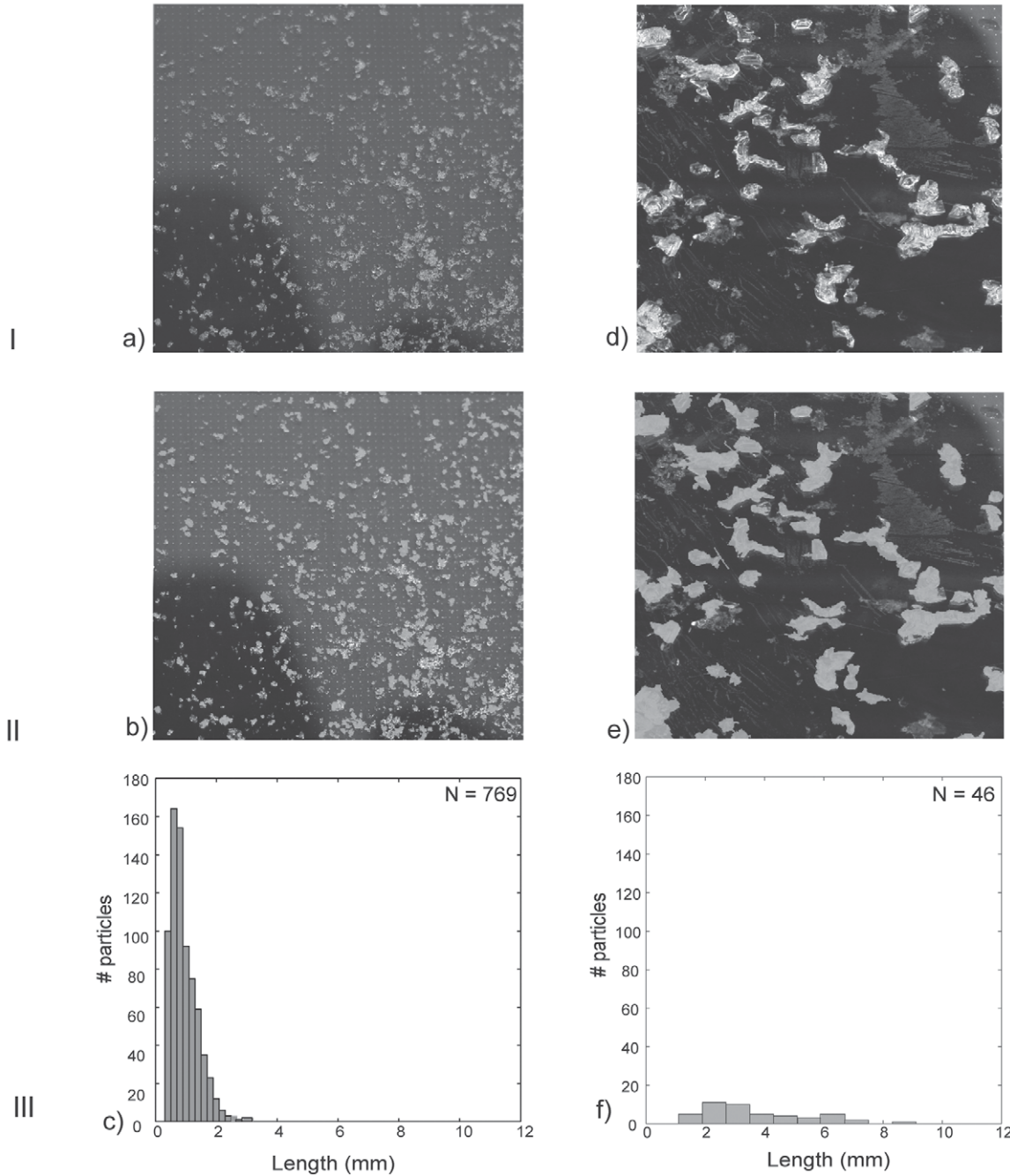| Sample	1	2
DSPP rule set	Järämä2	Järämä1
Grain type	Rounded grains	Depth hoar
Visual size	1 mm	4 mm
DSPP mean size	0.93 mm	3.74 mm
DSPP mode size	0.51 mm	2.33 mm

FIGURE 7. Snow grain images from Järämä in northern Sweden. The first column shows a sample of surface snow: (a) raw image; (b) classified image; and (c) resulting particle length distribution. The second column shows a sample identified as depth hoar: (d) raw image; (e) classified image; and (f) resulting particle length distribution. The values at the bottom of each column show in-field visually interpreted and DSPP-derived size values.
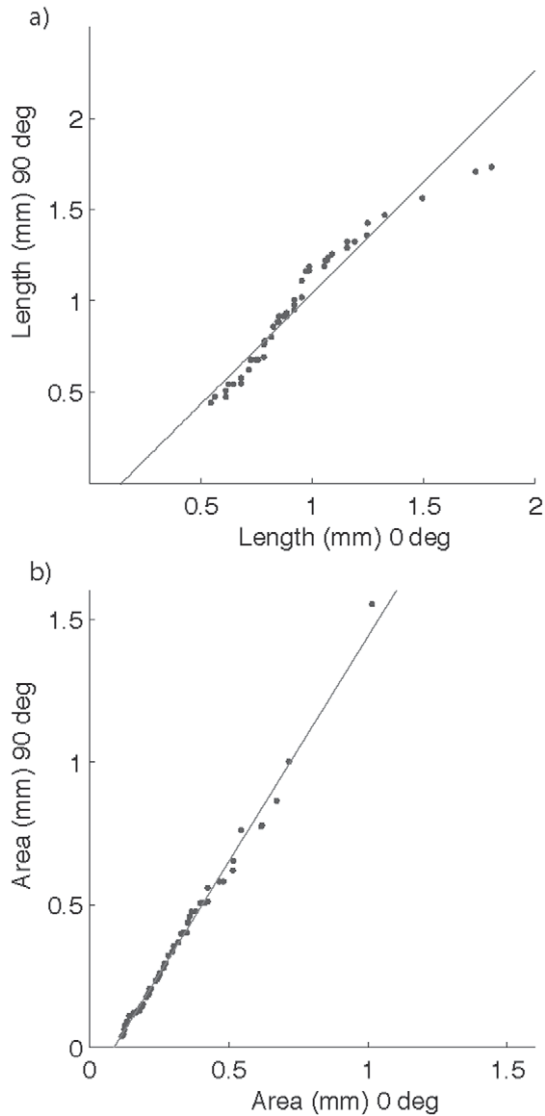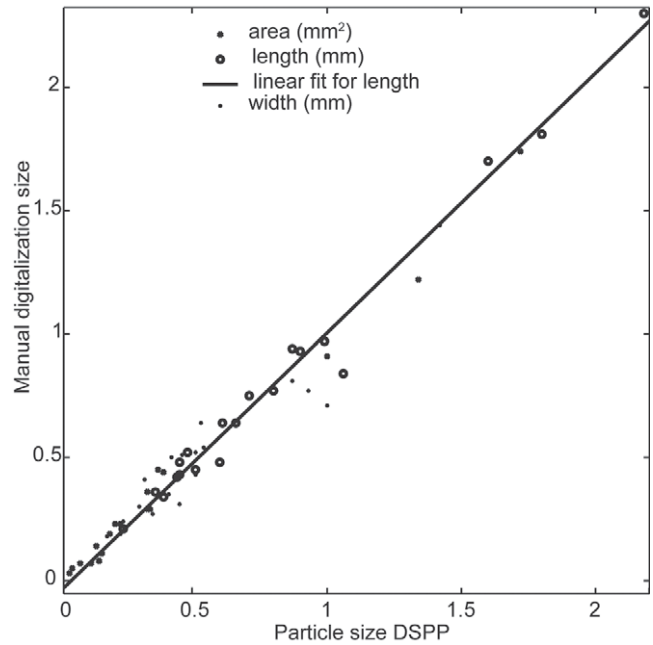
FIGURE 9. For validation purposes, images were digitized using visual interpretation (manual digitalization of particle size) and correlated using linear regression with the DSPP method for retrieved particle sizes (particle size DSPP). Twenty objects in four images were used for the analysis of the size parameters area, length, and width ($R^2 = 0.99$ and RMSE = 0.044 for area, $R^2 = 0.98$ and RMSE = 0.071 for length, and $R^2 = 0.91$ and RMSE = 0.089 for width).

FIGURE 8. Scatter plot of objects classified as snow particles in a test image before and after a 90° rotation for (a) particle length ($R^2 = 0.97$) and (b) particle area ($R^2 = 0.99$).

plies that the mean value may not be representative when analyzing snow grain size and should be taken into account when comparing to visual analysis of snow samples that usually provide average sizes. The primary advantages of the DSPP method are the range of descriptive statistics retrieved and the removal of visual subjective components of the snow particle size analysis. This allows users

TABLE 2

The resulting mean size in the three parameters (area [mm²], width [mm], and length [mm]) in an original example image and the results from a 90° shift of the same image.

Parameter (mean)	Original	90° shift
Area (mm²)	0.31	0.35
Length (mm)	0.91	0.93
Width (mm)	0.61	0.62

to apply the method widely. We would like to recommend that the nomenclature used in this paper be carefully considered so as to avoid confusion using the terms *particle* and *grain* in relation to what is actually studied.

The main limitation of the developed method is the two-dimensional analysis of three-dimensional natural snow objects. Furthermore, the georectification by pixel calculation reduces the accuracy, but this could be prevented by using a fixed distance between the camera and the sample grid. Melted snow particles (water droplets or refrozen water) resulting in clumping of particles affects the image analysis as they imitate the same classified features as the snow particles. This problem is reduced by using area, shape, and brightness limitations and by initial crop of the particle size images. Sufficient lighting conditions are also important to promote contrast in the image. The possibility exists that the morphology of the particles are altered by removal from the sampled snow; this error is not method specific and is considered to be marginal considering that the sample strategy is cautious and the particles are generally robust. An exception is fresh snow which has to be analyzed immediately when placed gently on the reference grid. The method facilitates the analysis of different types of snow (in shape and size) that occur in different regions with various physical settings. Large objects have a tendency to cluster and increase the mean size in the analysis. This effect is countered by manually cropping the image to remove clusters. This leads to fewer particles to be analyzed in each sample. We propose increasing number of parallel samples when analyzing larger particles in order to achieve a statistically reliable number of particles. The smallest particles also have a tendency to cluster due to their size (Ingvander et al., 2012).

The DSPP method is dynamic and can be tuned to account for differences in particle size and illumination. In the coastal region of Antarctica large particles were sampled under overcast conditions during the JASE traverse. The Järämä samples are separated into Järämä 1 and Järämä 2 rule sets in order to segment samples with small and large particles separately. The Tarfala samples were segmented with a scale parameter of 30 in order to capture fresh snow and small particles. The brightness threshold is considerably higher in the Tarfala classification, being an effect of sampling and photography performed in a 3-m-deep snow pit with poorer light conditions than surface sampling (i.e. overcast that generate whiteout and raise the general brightness level in the images). However, even in samples conducted with poor lighting conditions, the contrast between the snow particles and the background has proved to be sufficient for segmentation and classification.

Future development of the method is to establish constant elevation of the camera by fixing the reference grid plate to the tripod, which would generate constant resolution and higher accuracy in the images. Without tilt, the pixel resolution would be constant in the entire image and not be scattered as in Figure 3. However, the reference grid is also used for calculating camera distortion between the center and the border of the images [included in the process of Equation (1)], which we found negligible in this study, being less than 0.06 mm. Furthermore, photographing the snow fixed in its position would remove the possibility of grain alteration by movement. This would also provide information on how the particles are positioned against each other in the snow pack and small-scale information on the grain/air ratio within the snow. There are built in limitations in the software as the seed cells governing the multi-resolution segmentation grow in different directions depending on the angle of the image. This problem is overcome by photographing snow in its original position in the snow pack, which is a complicated but interesting next step for the DSPP method. The segmentation process was validated against manual delineation of snow particles (Fig. 9). This high accuracy is accomplished by the significant contrast in the image and high brightness of the particles. The segmentation process would induce larger errors on images with wider ranges in brightness of the snow particles and the background.

This method aims to provide accurate measurements of snow particles from large sample sizes in support of remote sensing investigations. The correlation of snow particle sizes with remote sensing observation is a work in progress. Here we show the potential of the DSPP method to derive size and shape measurements of snow particles in two dimensions; it should be noted that there are approaches that allow for the estimation of SSA from two-dimensional observations of snow particle size (e.g. Matzl and Schneebeli, 2010).

Conclusions

We have presented a method that combines rapid, simple data acquisition with sophisticated analysis for snow particle size assessment. The aim of the method was to improve upon the visual interpretation of snow particle size where project logistics could not cover refined instrumentation such as integrated sphere measurements of SSA or contact spectroscopy. As the DSPP method targets snow particles, i.e. bonded grains, as reflectors of radiation, the investigation does not aim to replace high-accuracy snow grain size analysis such as tomography or grain growth modeling (Schneebeli and Sokratov, 2004). However, the potential to retrieve

multiple two-dimensional size parameters enables further calculation of sizes on a subsample scale. The large number of samples that can be obtained offers statistical rigor not always found in snow particle size observations. In the future, evaluation against simultaneous measurements of DSPP photography and reliable measurements of specific surface area is desirable.

References Cited

Albert, M. R., 2002: Effects of snow on firn and ventilation on sublimation rates. *Annals of Glaciology,* 35: 52–56.

Baatz, M., and Schäpe, A., 2000: Multiresolution segmentation—An optimization approach for high quality multi-scale image segmentation. *In* Strobl, J., Blaschke, T., and Griesebner, G. (eds.), *Angewandte Geographische Informationsverarbeitung XII.* Karlsruhhe: Herbert Wichman, 12–23.

Benz, U., and Pottier, E., 2001: Object based analysis of polarimetric SAR data in alpha-entropy-anisotropy decomposition using fuzzy classification by eCognition. *Proceedings IGARSS 2003*, 4: 1913–1915.

Benz, U., Hofmann, P., Willhauck, G., Lingenfelder, I., and Heynen, M., 2004: Multi-resolution, object-oriented fuzzy analysis of remote sensing data for GIS-ready information. *ISPRS Journal of Photogrammetry and Remote Sensing*, 58: 239–258.

Brun, E., and Pahaut, E., 1991: An efficient method for delayed and accurate characterization of snow grains from natural snow packs. *Journal of Glaciology*, 37(127): 420–422.

Colbeck, S. C., 1998: Sintering in a dry snow cover. *Journal of Applied Physics,* 84(8): 4585–4589.

Colbeck, S. C., Akitaya, E., Armstrong, R., Gubler, H., Lafeuille, J., Lied, K., McKlung, D., and Morris, E., 1990: *The International Classification of Seasonal Snow on the Ground*. Wallingford, U.K.: The International Commission on Snow and Ice of the International Association of Scientific Hydrology, 23 pp.

Definiens, 2008: Definiens Developer 7.0 User Guide. Munich: Definiens AG.

Déry, S. J., and Yau, M. K., 2002: Large-scale mass balance effects of blowing snow and surface sublimation. *Journal of Geophysical Research*., 107(D23): http://dx.doi.org/10.1029/2001JD001251.

Domine, F., Albert, M., Hultwelker, T., Jacobi, H.-W., Kokhanovsky, A. A., Lehning, M., Picard, G., and Simpson, W. R., 2008: Snow physics as relevant to snow photochemistry. *Atmospheric Chemistry and Physics*, 8: 171–180.

Dozier, J., and Painter, T. H., 2004: Multispectral and hyperspectral remote sensing of alpine snow properties. *Remote Sensing of Environment*, 113: 525–527.

Dozier, J., Green, R. O., Nolin, A. W., and Painter, T. H., 2009: Interpretation of snow properties from imaging spectrometry. *Annual Review of Earth and Planetary Sciences*, 32: 465–494.

Fierz, C., Armstrong, R. L., Durand, Y., Etchevers, P., Greene, E., McClung, D. M., Nishimura, K., Satayawali, P. K., and Sokratov, S. A., 2009: *The International Classification for Seasonal Snow on the Ground.* Prepared by the ICSI-UCCS-IACS Working Group on Snow Classification. IHP-VII Technical Documents in Hydrology, UNESCO-IHP, N 83 IACS Contribution N1. Paris: UNESCO.

Fily, M., Bourdelles, B., Dedieu, J. P., and Sergent, C., 1997. Comparison of in situ and Landsat Thematic Mapper derived snow grain characteristics in the alps. *Remote Sensing of Environment*, 59: 452–460.

Fujii, Y., and Kusunoki, K., 1982: The role of sublimation and condensation in the formation of ice sheet surface at Mizuho Station, Antarctica. *Journal of Geophysical Research,* 87(C6): 4293–4300.

Gallet, J.-C., Domine, F., Zender, C. S., and Picard, G., 2009: Measurement of the specific surface area of snow using infrared reflectance in an integrating sphere at 1310 and 1550 nm. *The Cryosphere*, 3(2): 167–182.

Gay, M., Fily, M., Genthon, C., Frezzotti, M., Oerter, H., and Winther, J.-G., 2002: Snow grain-size measurements in Antarctica. *Journal of Glaciology,* 48(163): 167–182.

Grenfell, T., Warren, S. G., and Mullen, P. C., 1994: Reflection of solar radiation by the Antarctic snow surface at ultraviolet, visible and near-infrared wavelengths. *Journal of Geophysical Research*, 99(D9): 18,669–18,684.

Ingvander, S., Brown, I. A., and Jansson, P., 2010: Snow grain size variability along the JASE 2007/2008 traverse route in Droning Maud Land, Antarctica, and its relation to MOA NDSI index, MERIS and MODIS satellite data. ESA Special Publication, SP-686.

Ingvander, S., Johansson, C., Jansson, P., and Pettersson, R., 2012: Comparison between digital and manual methods of snow grain size estimation. *Hydrology Research*, 43(3): 192–202.

Ingvander, S., Rosqvist, G., Svensson, J., and Dahlke, H., 2013: Seasonal and interannual variability of elemental carbon in the snowpack of Storglaciären, northern Sweden. *Annals of Glaciology*, 54(62), 50–58, http://dx.doi.org/10.3189/2013AoG62A229.

Jacobi, H.-W., Domine, F., Simpson, W. R., Douglas, T. A., and Sturm, M., 2010: Simulations of the specific surface area of snow using one-dimensional physical snowpack model: implementation and evaluation for subarctic snow in Alaska. *The Cryosphere*, 4: 35–51.

Jansson, P., and Pettersson, R., 2007: Spatial and temporal characteristics of a long mass balance record, Storglaciären, Sweden. *Arctic, Antarctic, and Alpine Research*, 39(3): 432–437, http://dx.doi.org/10.1657/1523-0430(06-041)[JANSSON]2.0.CO;2.

Jansson, P., Linderholm, H. W., Pettersson, R., Karlin, T., and Mörth, C.-M., 2007: Assessing the possibility to couple chemical signals in winter snow on Storglaciären to atmospheric climatology. *Annals of Glaciology*, 46: 335–341.

Kärkäs, E., Granberg, H. B., Kanto, K., Rasmus, K., Lavoie, C., and Läppäranta, M., 2002: Physical properties of the seasonal snow cover in Dronning Maud Land, East Antarctica. *Annals of Glaciology*, 34: 89–94.

Kärkäs, E., Martma, T., and Sonninen, E., 2005: Physical properties and stratigraphy of surface snow in western Dronning Maud Land, Antarctica. *Polar Research*, 1–2: 55–67.

Kikuchi, T., Fukushima, Y., and Nishimura, K., 2005: Snow entrainment coefficient estimated by field observations and wind tunnel experiments. *Journal of Cold Regions Engineering,* 52: 309–315, http://dx.doi.org/10.1016/j.ijheatmasstransfer.2008.06.003.

Kirnbauer, R., Böschl, G., and Gutknecht, D., 1994: Entering the era of distributed snow models. *Nordic Hydrology*, 25: 1–24.

Legagneux, L., Cabanes, A., and Domine, F., 2002: Measurement of the specific surface area of 176 snow samples using methane adsorption at 77 K. *Journal of Geophysical* Research, 107(D17): 4335, http://dx.doi.org/10.1029/2001JD001016.

Lehning, M., Bartelt, P., Brown, R. L., Russi, T., Stöckli, U., and Zimmerli, M., 1999: Snowpack model calculations for avalanche warning based upon a new network of weather and snow stations. *Cold Regions Science and Technology*, 30(4): 145–157.

LeSaffre, B., Pougarch, E., and Martin, E., 1998: Objective determination of snow-grain characteristics from images. *Annals of Glaciology*, 26: 112–118.

Mätzler, C., 1996: Microwave permittivity of dry snow. *IEEE*, 34(2): 573–581.

Matzl, M., and Schneebeli, M., 2006: Measuring specific surface area of snow by near-infrared photography. *Journal of Glaciology*, 52(179): 558–564.

Matzl, M., and Schneebeli, M., 2010: Stereological measurement of the specific surface area of seasonal snow types: comparison to other methods, and implications for mm-scale vertical profiling. *Cold Regions Science and Technology*, 64(1): 1–8, http://dx.doi.org/10.1016/j.coldregions.2010.06.006.

Mellor, M., 1965: *Cold Regions Science and Engineering part III, Section A3c: Blowing Snow*. Hanover, New Hampshire: Cold Regions Research and Engineering Laboratory.

Neumann, T. A., Albert, M. R., Engel, C., Courville, Z., and Perron, F., 2009: Sublimation and the mass-transfer coefficient for snow sublimation. *International Journal of Heat and Mass Transfer*, 19(4): 117–129, http://dx.doi.org/10.1016/(ASCE)0887-381X(2005)19:4(117).

Nolin, A. W., and Dozier, J., 1993: Estimation snow grain size using AVIRIS data. *Remote Sensing of Environment*, 44: 231–238.

Nolin, A. W., and Dozier, J., 2000: A hyperspectral method for remotely sensing the grain-size of snow. *Remote Sensing of Environment*, 74: 207–216.

Painter, T. H., Molotch, N. P., Cassidy, M., Flanner, M., and Steffen, K., 2007: Contact spectroscopy for determination of stratigraphy of snow optical grain size. *Journal of Glaciology*, 53(180): 121–127.

Painter, T. H., Rittger, K., McKenzie, C., and Slaughter, P., 2009: A retrieval of subpixel snow covered area, grain size and albedo from MODIS. *Remote Sensing of Environment*, 113: 868–879.

Perla, R., 1982: Preparation of section planes in snow specimens. *Journal of Glaciology*, 28(98): 199–204.

Picard, G., Arnaud, L., Domine, F., and Fily, M., 2009: Determining snow specific surface area from near-infrared reflectance measurements: numerical study of the influence of grain shape. *Cold Regions Science and Technology,* 56: 10–17.

Pulliainen, J., 2006: Mapping of snow water equivalent and snow depth in boreal and sub-arctic zones by assimilating space-borne microwave radiometer data and ground-based observations. *Remote Sensing of Environment*, 101: 257–269.

Rolland du Roscoat, S., King, A., Philip, A., Reischig, P., Ludwig, W., Flin, F., and Meyssonnier, J., 2011: Analysis of snow microstructure by means of X-ray diffraction contrast tomography. *Advanced Engineering Materials*, 13(3): 128–135, http://dx.doi.org/10.1002/adem.201000221.

Scambos, T. A., Haran, T. M., Fahnestock, M. A., and Painter, T. H., 2007: MODIS-based mosaic of Antarctica (MOA) data sets: continent-wide surface morphology and snow grain size. *Remote Sensing of Environment*, 111: 242–257.

Schiewe, J., 2002. Segmentation of high-resolution remotely sensed data—Concepts, applications and problems. *International Archives of Photogrammetry Remote Sensing,* 34 (4): 380–385.

Schneebeli, M., and Sokratov, S. A., 2004: Tomography of temperature gradient metamorphism of snow and associated changes in heat conductivity. *Hydrological Processes*, 18: 3655–3665, http://dx.doi.org/10.1002/hyp.5800.

Sommerfeld, R. A., and LaChapelle, E., 1970: The classification of snow metamorphism. *Journal of Glaciology*, 9(55): 3–17.

van der Sande, C. J., de Jong, S. M., and de Roo, A. P. J., 2003: A segmentation and classification approach of IKONOS-2 imagery for land cover mapping to assist flood risk and flood damage assessment. *International Journal of Applied Earth Observation and Geoinformation*, 4: 217–229.

Wiscombe, W. J., and Warren, S. G., 1980: A model for the spectral albedo of snow. *Journal of Atmospheric Science*, 37: 2712–2733.